Cancer Biomarkers -1 (2024) 1–17
DOI 10.3233/CBM-230489
IOS Press
CORRECTED PROOF

Identification of RNA-binding protein RBMS3 as a potential biomarker for immunotherapy in bladder cancer

Tarimo Fredrick Praygod[a,1], Jinlong Li[b,1], Hongwei Li[b], Wanlong Tan[a,*], Zhiming Hu[b,*] and Li Zhou[c,d,*]

[a]*Department of Urology, Nanfang Hospital, Southern Medical University, Guangzhou, Guangdong, China*
[b]*Institute of Biotherapy, School of Laboratory Medicine and Biotechnology, Southern Medical University, Guangzhou, Guangdong, China*
[c]*Institute of Interdisciplinary Research, Guangdong Polytechnic Normal University, Guangzhou, Guangdong, China*
[d]*Research Institute of Guangdong Polytechnic Normal University in Heyuan City, Guangdong, China*

Received 14 November 2023
Accepted 15 July 2024

Abstract. RNA-binding protein (RBP) plays pivotal roles in the malignant progression of cancer by regulating gene expression. In this paper, we aimed to develop RBP-based prognostic signature and identify critical hub RBPs in bladder cancer (BLCA). Firstly, a risk model based on differentially expressed RBP gens (DERBPs) between normal and tumor tissues was successfully established, which can predict the tumor stromal score and drug sensitivity. Then two another RBP risk models based on miRNA-correlated RBPs or lncRNA-correlated RBPs were also established, and *RBMS3* was identified as the overlapping gene in the three models. Data from multiple bioinformatics databases revealed that *RBMS3* was an independent prognostic factor for overall survival (OS), and was associated with an immunosuppressive tumor microenvironment (TME) in BLCA. Further, Single-cell RNA-Seq (scRNA-Seq) data and the human protein altas (HPA) database showed that RBMS3 expression (both mRNA and protein) were up-regulated in BLCA tumor and tumor stromal cells. Finally, *RBMS3* was shown to be associated with worse response to BLCA immunotherapy. Overall, RBMS3 is a key prognostic RBP with TME remodeling function and may serve as a target for BLCA immunotherapy.

Keywords: RNA-binding protein, RBMS3, immunosuppressive tumor microenvironment, bladder cancer

1. Introduction

Bladder cancer (BLCA) is the fourth-most common malignant disease in men and the ninth most common cancer in women. It accounts for an estimated 573,000 new cases and 213,000 deaths annually worldwide [1]. According to the depth of bladder wall invasion, BLCA can be categorized as non-invasive papillary carcinoma (Ta) or as a tumor invading the lamina propria (T1), muscles (T2), or beyond (T3, T4). Ta and T1 are also classified as non–muscle-invasive BLCA and are treated differently from tumors that invade the muscle or beyond [2]. Based on their large-scale messenger RNA (mRNA) expression profiles, human cancers can be grouped into molecular subtypes, which share similar gene-expression patterns and biological characteristics. BLCA can be categorized into basal and luminal molecular subtypes, which can inform clinical behaviors like the response to neoadjuvant chemotherapy, the sensitivity to immunotherapy, and the risk of pro-

[1]Authors contributed equally to this work.

*Corresponding authors: Li Zhou, Institute of Interdisciplinary Research, Guangdong Polytechnic Normal University, 293 Zhongshan Avenue West, Tianhe District, Guangzhou, China. E-mail: zhouli@gpnu.edu.cn. Zhiming Hu, School of Laboratory Medicine and Biotechnology, Southern Medical University, 1023 Sha Tai Road, Guangzhou, Guangdong 510515, China. E-mail: hzm@smu.edu.cn. Wanlong Tan, Department of Urology, Nanfang Hospital, Southern Medical University, 1838 North of Guangzhou Avenue, Baiyun, Guangzhou, Guangdong 510515, China. E-mail: twl@smu.edu.cn.

gression [3]. Recently, the risk stratification of BLCA has been made more accurate and personalized by integrating tumor genetic-sequencing data with clinical outcomes [4]. This provides a basis for determining the most appropriate treatment regimen for BLCA, such as whether neoadjuvant chemotherapy should be administered prior to radical cystectomy or not [4]. In the future, risk classification, including molecular subtyping with specific treatment considerations, will provide great assistance in the clinical management of BLCA [4].

RNA-binding proteins (RBPs) interact with various classes of RNAs, including mRNA, long non-coding RNA (lncRNA), and transfer RNA to form ribonucleoprotein complexes. This enables them to play pivotal roles in the regulation of gene expression at the post-transcriptional level [5]. To date, more than 1500 RBPs have been identified, representing approximately 7.5% of all protein-coding genes in the human genome [6]. Dysregulation of RBPs is associated with various diseases. In cancers, RBP modulates the expression of target RNAs involving in various cellular processes like proliferation, angiogenesis, senescence, and metastasis [7]. Many recent studies have shown that RBPs can regulate TME constitution and hence influence cancer progression in various types of cancer such as colorectal cancer [8], gastric cancer [9], hepatocellular cancer [10] and bladder cancer [11] . This indicates RBPs a potential target for TME-based anticancer therapy.

Many studies have reported risk signatures based on RBP expression in various types of tumors, such as hepatocellular carcinoma [12], lung cancer [13], osteosarcoma [14], head and neck carcinoma [15], and liver cancer [16]. In BLCA, risk signatures composed of six RBPs [17], eight RBPs [18], and 12 RBPs [19] have been reported to have predictive value for overall survival (OS). However, those risk signatures contained too many member genes and its clinical application were therefore limited. Moreover, most studies did not perform further analysis of these RBP molecules, such as identifying the source of the RBP, exploring its relationship with the tumor microenvironment (TME). Therefore, in this study, we first identified prognostic RBP signatures based on three data profiles: the differentially expressed RBPs between normal and BLCA tissues and the miRNA-correlated and lncRNA-correlated RBPs with prognostic value in BLCA cancer tissues. The critical prognostic RBP members was identified by intersection of the three signatures, and RBMS3 was ultimately selected as the unique gene present in all three signatures. Further analysis demonstrated that high RBMS3 expression was associated with greater stromal content and predicted poor survival after immunotherapy.

2. Materials and methods

2.1. Data acquisition and processing

Bulk RNA-sequencing (RNA-Seq) data (19 normal, 412 tumors), microRNA (miRNA) data (19 normal, 418 tumors) and clinical information were downloaded from the TCGA-BLCA database (https://portal.gdc.cancer.gov). A total of 1836 genes encoding human RBPs were summarized from the RNA-binding Protein Database [20] and published literature [5,21,22]. The mRNA matrix of the 1836 RBP genes was extracted, and the differentially expressed RBP genes (DERBPs) were obtained by using the "edgeR" R package, with thresholds $|\log2FC| > 1.0$, $P < 0.05$, and false-discovery rate (FDR) < 0.05. The correlation between RBP expression and miRNA or lncRNA concentrations was analyzed using the correlation test function of R (in the "limma" R package), ultimately identifying 266 miRNA-correlated RBPs and 268 lncRNA-correlated RBPs.

2.2. Construction and validation of prognostic RBP signatures

The DERBPs, miRNA-correlated RBPs or lncRNA-correlated RBPs were respectively subjected to univariate Cox regression analysis using the "survival" R package to identify the genes that significantly affected the OS ($P < 0.05$). Multivariate Cox regression analysis was used to construct the prognostic signatures. Hazard ratios (HRs) and regression coefficients were calculated for each gene. The risk score for each patient was calculated using the following equation:

$$\text{Risk score} = \sum_{i=1}^{N} \beta i \times Ei$$

Where N represents the total number of signature genes and βi and *Ei* represent the coefficient index and gene-expression value of each gene, respectively.

The patients were sorted into high- and low-risk groups based on the median risk score. The risk score model, survival status, and expression levels of the signature genes in TCGA-BLCA cancer patients were generated by the "pheatmap" R package. A receiver operating characteristic (ROC) curve was generated using the "survival" R package. The Kaplan–Meier survival curves of high- and low-risk patients were generated using the "survminer" R package.

2.3. Construction of the nomogram

To assess the probability of OS in BLCA at 1, 3, and 5 years, a nomogram combining clinical characteristics and the risk score was constructed using the "rms" R package. Calibration plots were used to evaluate the discriminative ability of the nomogram.

2.4. Evaluation of tumor stromal score and immune cell infiltration

The ESTIMATE stromal and immune scores of TCGA-BLCA patients were calculated using the "ESTIMATE" R package and visualized by the "ggpubr" R package. The infiltration of 22 immune cells was analyzed by the "CIBERSORT" R package. Differences in various immune cell components between the high- and low-risk groups were analyzed by the "limma" R package and visualized by the "ggplot2" R package. The immune checkpoint genes were sourced from previously published literature [23,24], and their different expression between the high- and low-risk groups was analyzed by the "limma" R package. Tumor purity and the correlation between gene expression and immune cell infiltration were analyzed using the Tumor Immune Estimation Resource (TIMER2.0) (http://timer.cistrome.org).

2.5. Correlation analysis of RBMS3 expression and gene signatures

Correlation analysis between *RBMS3* and gene signatures of various cells, including effector regulatory T-cells (*FOXP3, CTLA4, CCR8, TNFRSF9*), exhausted T-cells (*HAVCR2, TIGIT, LAG3, PDCD1, CXCL13, LAYN*), fibroblasts *(RGS5, COL1A1, PDGFRA, PDGFRB, DES*), and endothelial cells (*VWF, PECAM1*) in the TCGA-BLCA dataset was performed using gene-expression profiling interactive analysis (GEPIA2) (http://gepia2.cancer-pku.cn) [25].

2.6. scRNA-Seq data preprocessing

The scRNA-Seq data GSE190888, including one case of cystitis glandularis, one case of low-grade BLCA, one case of high-grade BLCA, and one case of recurrent BLCA, and the scRNA-Seq data GSE192575, including one case of chemotherapy-sensitive and one case of chemotherapy-resistant human bladder cancers, were obtained from the Gene Expression Omnibus database. The scRNA-Seq data were processed using the "seurat" R package. Cells with 300 genes at least and mitochondrial genes $< 10\%$ were selected. The top 2,000 variably expressed genes were selected using the FindVariableFeatures function to perform principal component analysis. Cell-clustering analysis was performed using a t-distributed stochastic neighbor embedding (tSNE) scheme. Marker genes were selected according to $|\log2FC| > 1.0$ and adjusted $P < 0.01$. Cell annotation was facilitated using the R package "SingleR".

2.7. Evaluation of the predictive ability of RBMS3 on BLCA immunotherapy

The immunotherapy datasets were obtained from IMvigor210CoreBiologies (http://research-pub.gene.com/IMvigor210CoreBiologies/packageVersions/). Patients with complete remission (CR) or partial response (PR) were classified as response (R), and those with stale disease (SD) or progressive disease (PD) were classified as non-response (NR). Patients were divided into high- and low-expression groups according to *RBMS3* expression level to analyze the its relationship with immunotherapy efficacy and OS. Additionally, the predictive ability of RBMS3 for immunotherapeutic OS was analyzed through the Kaplan-Meier Plotter (https://kmplot.com).

2.8. Quantitative real-time PCR and immunohistochemistry (IHC)

Bladder cancer tissues were obtained from patients who had undergone surgical resection at Southern Medical University (Guangzhou, China) with consent from all patients. The experimental protocols were approved by the ethics committee of Southern Medical University. Trizol reagent (TaKaRa, Kusatsu, Japan) was used to extract total RNA from BLCA specimens according to the manufacturer's protocol. Reverse transcription and quantitative real-time PCR were performed as described before [26], with the primers as follow. RBMS3 forward primer: 5'-CAGTGGACACATCCAACGAAC-3', reverse primer: 5'-CTTCTTGTTCAATGAAGTTTCTTC-3'. GAPDH forward primer: 5'-AGCCACATCGCTCAGACAC-3', reverse primer: 5'-GCCCAATACGACCAAATCC-3'. The expression levels of *RMBS3* mRNA were normalized using the GAPDH expression. Each assay reaction was performed in triplicate.

The bladder cancer tissues were subjected to IHC analysis as routine. Briefly, the bladder cancer tissues

were sequentially fixed (4% paraformaldehyde), paraffin embedded, paraffin sections (4–5 μm) deparaffinized and rehydrated, and antigen recovered. After blocking, the sections were sequentially incubated with anti-RBMS3 Rabbit Ab (Abcam, ab272612) and the second biotinylated antibody. Nuclei were counterstained with hematoxylin. Anti-rat Ig SABC assay kit (spring) was used to observe positively expressed proteins.

2.9. Statistical analysis

R software version 4.2.2 (R Foundation for Statistical Computing, Vienna, Austria) (http://www.R-project.org) was used for statistical analyses. The packages within R were used as described above. Wilcoxon test was used to compare *RBMS3* expression between the different response groups (NR vs. R). Chi-square-test was used to compare the fraction of response in high- and low-*RBMS3* groups. Kaplan-Meier method was used for survival analysis. $P < 0.05$ was considered statistically significant.

3. Results

3.1. Identification of DERBPs

A total of 111 DERBPs between the normal and tumor groups were identified, of which 56 were downregulated and 55 were upregulated in BLCA tissues (Fig. 1A, B, Supplementary Fig. 1). In GO analysis, RNA catabolic processes, regulation of mRNA metabolic process and regulation of translation were highly enriched (Fig. 1C). In each category, both upregulated and downregulated DERBPs were enriched, whereas, in the RNA catabolic process, more DERBPs were downregulated in cancer tissues (Fig. 1C). KEGG analysis showed that miRNAs in cancer, platinum drug resistance, influenza A, and mRNA surveillance pathways were upregulated in cancer tissues (Fig. 1D).

3.2. Construction and verification of the prognostic signature based on the DERBPs

26 genes were identified with statistical prognostic significance with univariate Cox regression analysis ($P < 0.05$) (Fig. 2A). Further, ten most powerful prognostic genes (*CTIF, RBMS3, PPARGC1B, PABPC1L, HIST1H1C, DARS2, FASN, EPPK1, RPS10, RPP21*) were screened out by a multivariate Cox regression to construct a risk score model. According to the median risk score, the BLCA cancer samples were divided into low- and high-risk groups (Fig. 2B). A significant difference was noted in survival probability between the low- and high-risk groups ($P < 0.001$) (Fig. 2C). Univariate (Fig. 2D) and multivariate (Fig. 2E) Cox regression analyses indicated that the risk score was an independent prognostic factor for BLCA patients ($P < 0.001$). The risk score predicted 1, 3, and 5-year OS with an area under the ROC curve of > 0.75, suggesting optimal specificity and sensitivity for prognostic evaluation (Fig. 2F). Finally, a nomogram including age, gender, T/M/N, and risk score was successfully constructed (Fig. 2G). The calibration plots for 1-, 3- and 5-year OS showed that the nomogram model demonstrated better prognostic prediction (Fig. 2H).

3.3. The prognostic signature is associated with higher tumor stromal scores and predicts chemotherapy sensitivity

GSEA analysis was performed to detect the vital tumor phenotypes correlated with the risk score. It showed that genes related to adhesion, junction, ECM-receptor interaction, and canonical TME-related signal pathways like TGFβ, WNT, VEGF were enriched in the high-risk group (Fig. 3A, Supplementary Tables 1, 2), suggesting a different TME phenotype. Consistently, the high-risk group demonstrated higher ESTIMATE and stromal scores than the low-risk group ($P < 0.001$); however, there was no significant difference in immune scores between the two groups (Fig. 3B). To further clarify the correlation between the risk score and immune landscape, differences in various immune cell components between the two groups were analyzed using CIBERSORT.R. The high-risk group showed greater neutrophil ($P < 0.01$) and M0 and M2 macrophage ($p < 0.05$) counts. Fractions of most of the 22 kinds of immune cells, including $CD4^+$T, $CD8^+$T, follicular helper T, NK, and dendritic cells, were reduced in the high-risk group, but the difference was not statistically significant (Fig. 3C). Further, several immune checkpoint genes were upregulated in the high-risk group (Fig. 3D), indicating an immunosuppressive microenvironment. These results indicate that the prognostic RBPs may be involved in stromal abundance and regulation of the immune microenvironment.

TME plays essential roles in the efficiency of cancer therapy. To evaluate the potential value of the risk signature to predict response to clinical drug therapy, estimated IC_{50} of 198 drugs was analyzed by the "OncoPredict" R package. As expected, the prog-

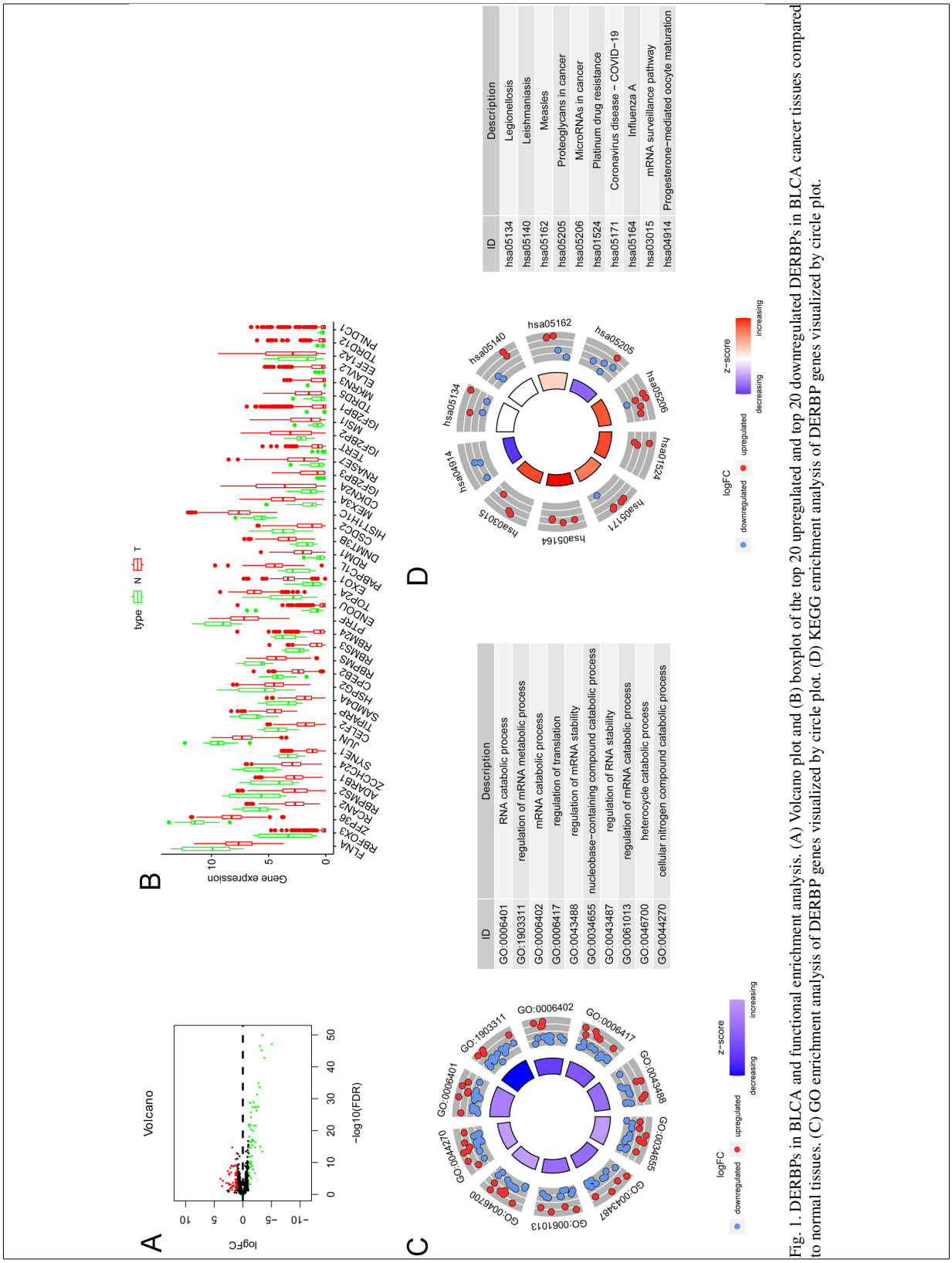

ID	Description
GO:0006401	RNA catabolic process
GO:1903311	regulation of mRNA metabolic process
GO:0006402	mRNA catabolic process
GO:0006417	regulation of translation
GO:0043488	regulation of mRNA stability
GO:0034655	nucleobase−containing compound catabolic process
GO:0043487	regulation of RNA stability
GO:0061013	regulation of mRNA catabolic process
GO:0046700	heterocycle catabolic process
GO:0044270	cellular nitrogen compound catabolic process

ID	Description
hsa05134	Legionellosis
hsa05140	Leishmaniasis
hsa05162	Measles
hsa05205	Proteoglycans in cancer
hsa05206	MicroRNAs in cancer
hsa01524	Platinum drug resistance
hsa05171	Coronavirus disease − COVID−19
hsa05164	Influenza A
hsa03015	mRNA surveillance pathway
hsa04914	Progesterone−mediated oocyte maturation

Fig. 1. DERBPs in BLCA and functional enrichment analysis. (A) Volcano plot and (B) boxplot of the top 20 upregulated and top 20 downregulated DERBPs in BLCA cancer tissues compared to normal tissues. (C) GO enrichment analysis of DERBP genes visualized by circle plot. (D) KEGG enrichment analysis of DERBP genes visualized by circle plot.

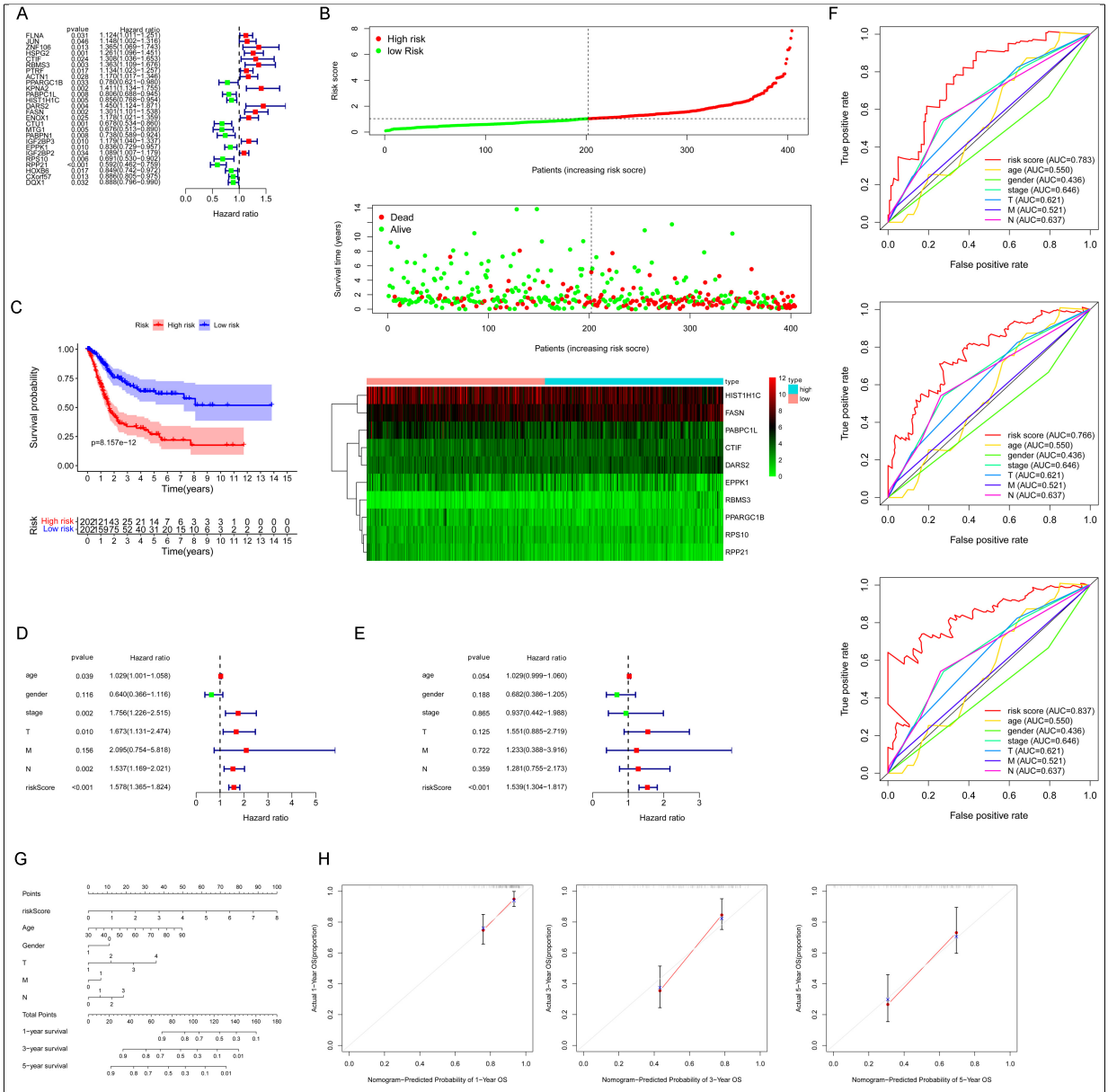

Fig. 2. Construction and verification of the prognostic DERBP signature. (A) Survival-related DERBPs were obtained by univariate Cox regression, $P < 0.05$. The prognostic DERBPs were visualized by forest plot. (B) Risk score model, survival status, and expression levels of the 10 signature genes in TCGA-BLCA cancer patients. (C) Kaplan–Meier survival analysis of TCGA-BLCA cancer patients based on risk score. (D) Univariate Cox regression and (E) multivariate Cox regression analysis of the risk score and different clinical features. (F) ROC curves demonstrated the predictive prognostic value of risk score at 1, 3, and 5 years. (G) Nomogram consisting of age, gender, T/M/N, and risk score based on the 10 hub DERBPs. (H) Calibration curve for validation of the nomogram for estimating patient survival at 1, 3, and 5 years.

nostic signature was associated with chemotherapy sensitivity. High-risk group was less sensitive to Oxaliplatin_1089, Acetalax_1804, and Lapatinib_1558; but sensitive to certain kind of inhibitors, such as IGF1R/IR inhibitor BMS-754807, pan-kinase inhibitor Staurosporine_1034, and heat shock protein 90 inhibitor Luminespib_1559 (Fig. 3E).

3.4. RBMS3 is the critical hub gene with prognostic value in BLCA

RBPs exert biological functions mainly by regulating target RNA. To further explore the critical RBPs for cancer development, the correlation between RBPs and RNA expression (miRNA and

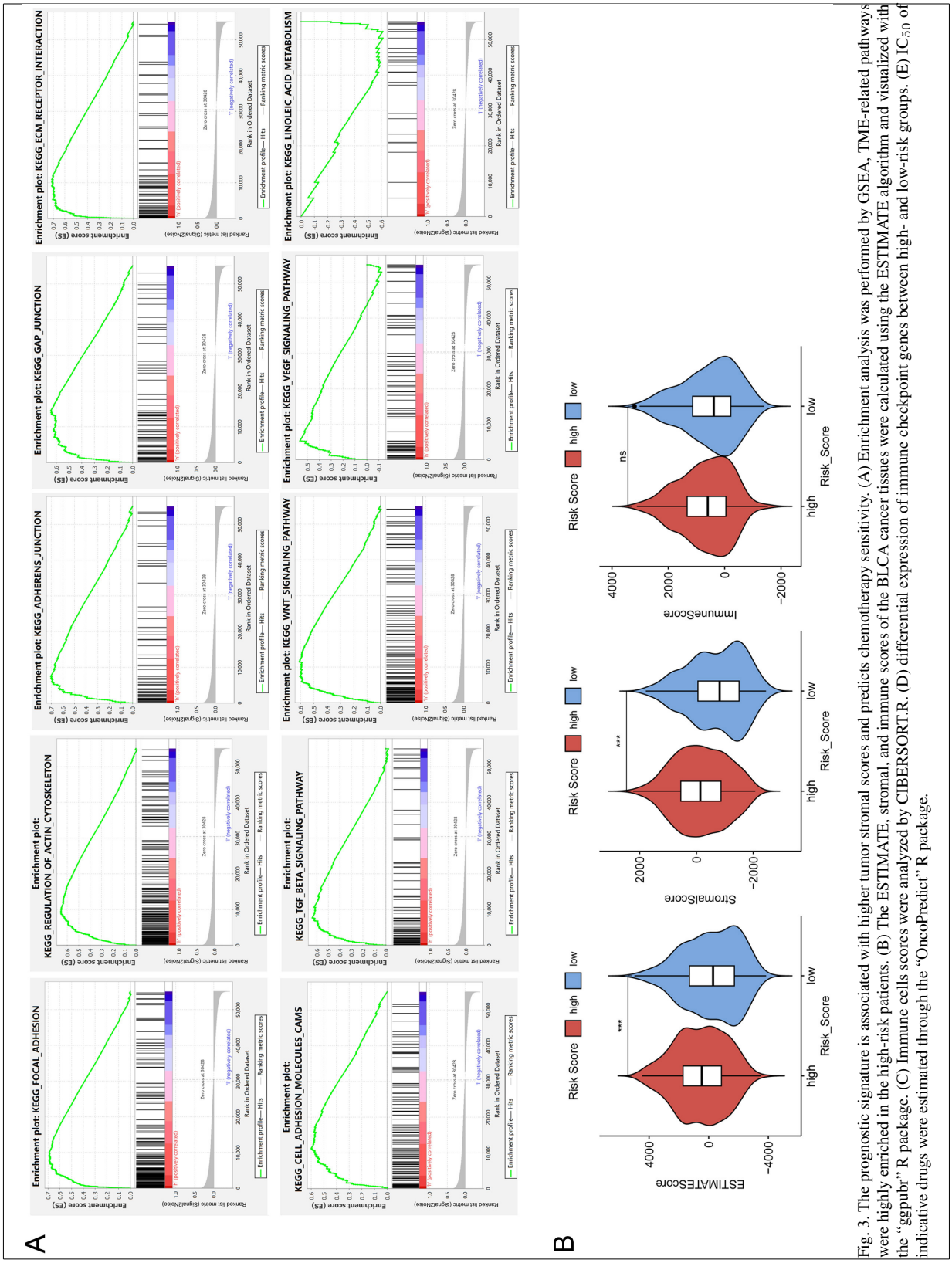

Fig. 3. The prognostic signature is associated with higher tumor stromal scores and predicts chemotherapy sensitivity. (A) Enrichment analysis was performed by GSEA, TME-related pathways were highly enriched in the high-risk patients. (B) The ESTIMATE, stromal, and immune scores of the BLCA cancer tissues were calculated using the ESTIMATE algorithm and visualized with the "ggpubr" R package. (C) Immune cells scores were analyzed by CIBERSORT.R. (D) differential expression of immune checkpoint genes between high- and low-risk groups. (E) IC_{50} of indicative drugs were estimated through the "OncoPredict" R package.

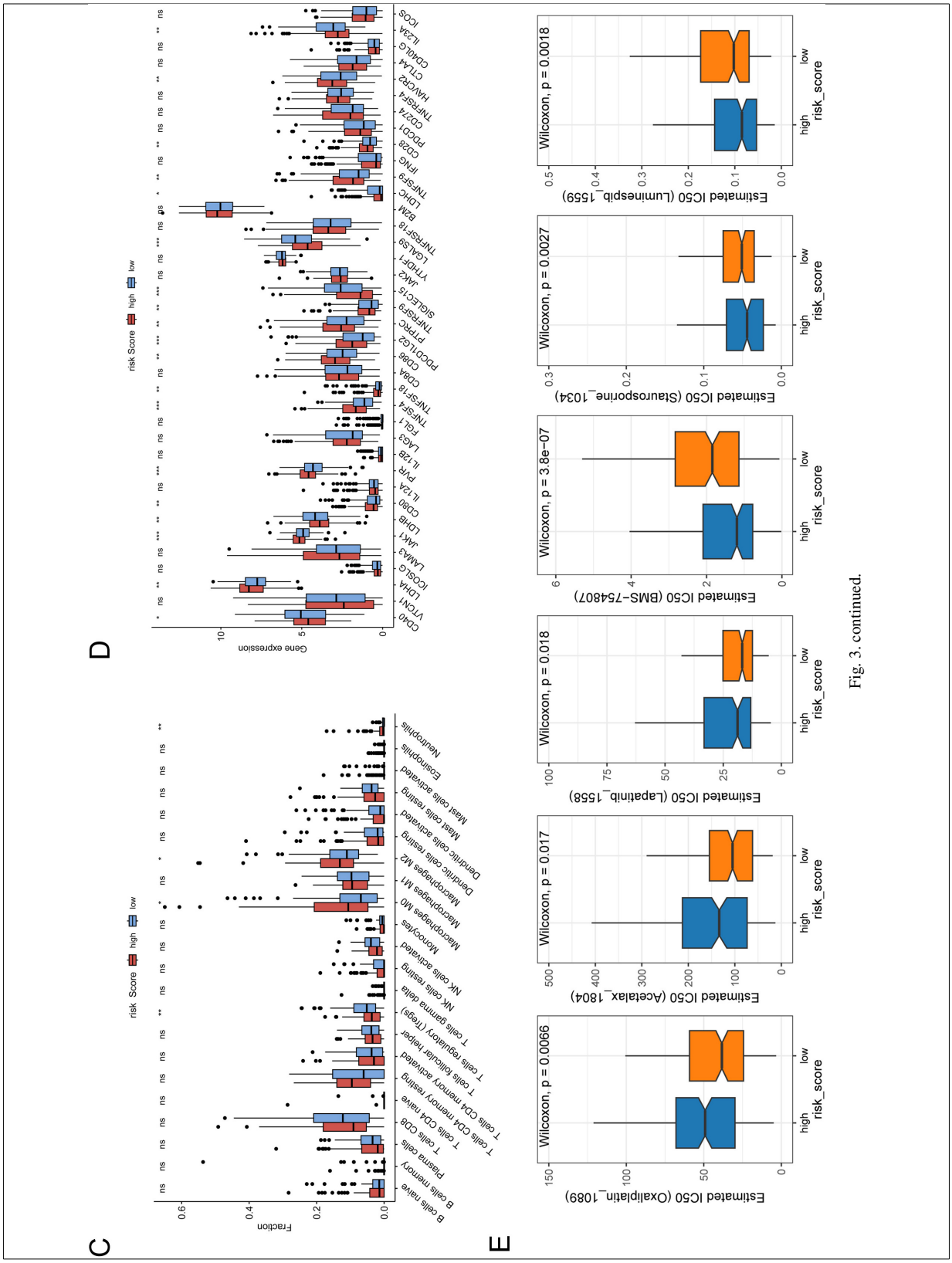

Fig. 3. continued.

lncRNA) in BLCA was analyzed to obtain RNA-correlated RBPs, from which risk models were constructed. Six miRNA-correlated RBPs (*CTU1, MYO5A, OAS1, PATL2, RBMS3, TXNL4A*) and seven lncRNA-correlated RBPs (*DDX39B, EIF4B, ELAC1, MYO5A, PATL2, RBMS3, TIA1*) were finally screened out as prognostic risk genes (Fig. 4A, Supplementary Fig. 2). To narrow down the number of prognostic RBPs, three RBP prognostic signatures (miRNA-correlated RBPs, lncRNA-correlated RBPs, and DERBPs) were intersected to identify the overlapping genes. *RBMS3* was a unique gene found in all three signatures (Fig. 4B), strongly suggesting that RBMS3 is a critical RBP for BLCA development.

Next, the expression profile of *RBMS3* in BLCA was analyzed using GEPIA2. Surprisingly, *RBMS3* was significantly downregulated in BLCA cancer tissues, compared to normal tissues which including TCGA normal and the Genotype-Tissue Expression (GTEx) bladder data (Fig. 4C). However, in tumor tissues, *RBMS3* expression was positively correlated with tumor stage (Fig. 4D). Moreover, *RBMS3* was a risk factor for OS; high *RBMS3* expression alone could predict poor survival of BLCA. High *RBMS3* expression was a risk factor in papillary BLCA (HR = 2.2, $P = 0.016$) (Fig. 4E), but not significant in non-papillary BLCA (HR = 1.3, $P = 0.093$) (Fig. 4E). The correlation between *RBMS3* mRNA expression and OS was further explored using the Kaplan-Meier Plotter. High *RBMS3* expression was correlated with shorter OS in BLCA (HR = 1.83, $P = 0.00048$). More importantly, tumor stage-restricted analysis showed that high RBMS3 levels were correlated with shorter OS in stage IV patients. However, among patients with lower tumor stages (stages II and III), the OS was not statistically different (Fig. 4F). These results indicate that RBMS3 may contribute to the malignant progression of BLCA.

3.5. *RBMS3 is associated with high tumor matrix content and immunosuppressive environment*

The correlation between *RBMS3* expression, tumor purity, and immune cell infiltration was analyzed using TIMER2. High *RBMS3* expression was associated with lower tumor purity (R = -0.465, $P < 0.001$) and was positively correlated with infiltration by neutrophils (R = 0.37, $P < 0.001$), dendritic cells (R = 0.312, $P < 0.001$), endothelial cells (R = 0.326, $P < 0.001$), and cancer associated fibroblast (R = 0.496, $P < 0.001$) (Fig. 5A). The correlation between *RBMS3* expression and stromal cells was further explored using GEPIA2, revealing that *RBMS3* expression was highly correlated with fibroblast markers (R = 0.65, $P < 0.001$), as well as endothelial cell markers (R = 0.51, $P < 0.001$). More importantly, *RBMS3* expression was positively correlated with exhausted T-cells (R = 0.51, $P < 0.001$) and effector regulatory T-cells (R = 0.47, $P < 0.001$) (Fig. 5B). These results indicate that RBMS3 correlates with high tumor stromal content and associated with an immunosuppressive environment.

3.6. *RBMS3 is mainly expressed in tumor, endothelial, and fibroblast cells in BLCA tissues*

To characterize *RBMS3* expression, scRNA-Seq data (GSE190888) of patients with cystitis and BLCA were analyzed. After quality control, 3179 cells with cystitis, 5376 cells with high-grade BLCA, 4583 cells with low-grade BLCA, and 4885 cells with recurrent BLCA were obtained. According to tSNE and cell-type annotation, the cells were clustered into the following six groups: epithelial, endothelial, T/NK, B-, macrophage, and fibroblast cells (Fig. 6A, B). *RBMS3* was mainly expressed in epithelial, endothelial, and fibroblast cells but rarely in immune cells (Fig. 6C). This is consistent with the above data on the correlation of *RBMS3* with tumor stroma. Furthermore, *RBMS3* expression was increased in recurrent patients, especially in recurrent fibroblasts (Fig. 6D). Moreover, in another scRNA-Seq data (GSE192575) which containing chemotherapy-sensitive and resistant human bladder cancers, the expression of *RBMS3* was significantly increased in the chemotherapy-resistant bladder cancer (Supplementary Fig. 3). This indicates that RBMS3 may be involved in activating cancer-associated fibroblasts and could contribute to TME remodeling.

To further clarify RBMS3 expression at protein level, the Human Protein Atlas database was searched to compare expression levels between normal bladder and BLCA tissues. RBMS3 protein was expressed at a moderate intensity in 75%–25% of normal bladder tissues. RBMS3 expression showed significant heterogeneity in BLCA tissues. It varied from weak to moderate to strong among the different tumor tissues (Fig. 7). More importantly, RBMS3 was not ubiquitously expressed in tumor tissues. In most tumors, only a portion ($< 25\%$) of the tumor cells expressed high levels of RBMS3. Notably, in some patients, high levels of RBMS3 were observed in the tumor stromal area (Fig. 7A). Further, we compared the RBMS3 expression between primary and recurrent BLCA tissues. It showed that both mRNA and protein level of RBMS3 was significantly increased in the recurrent BLCA tissue (Fig. 7B).

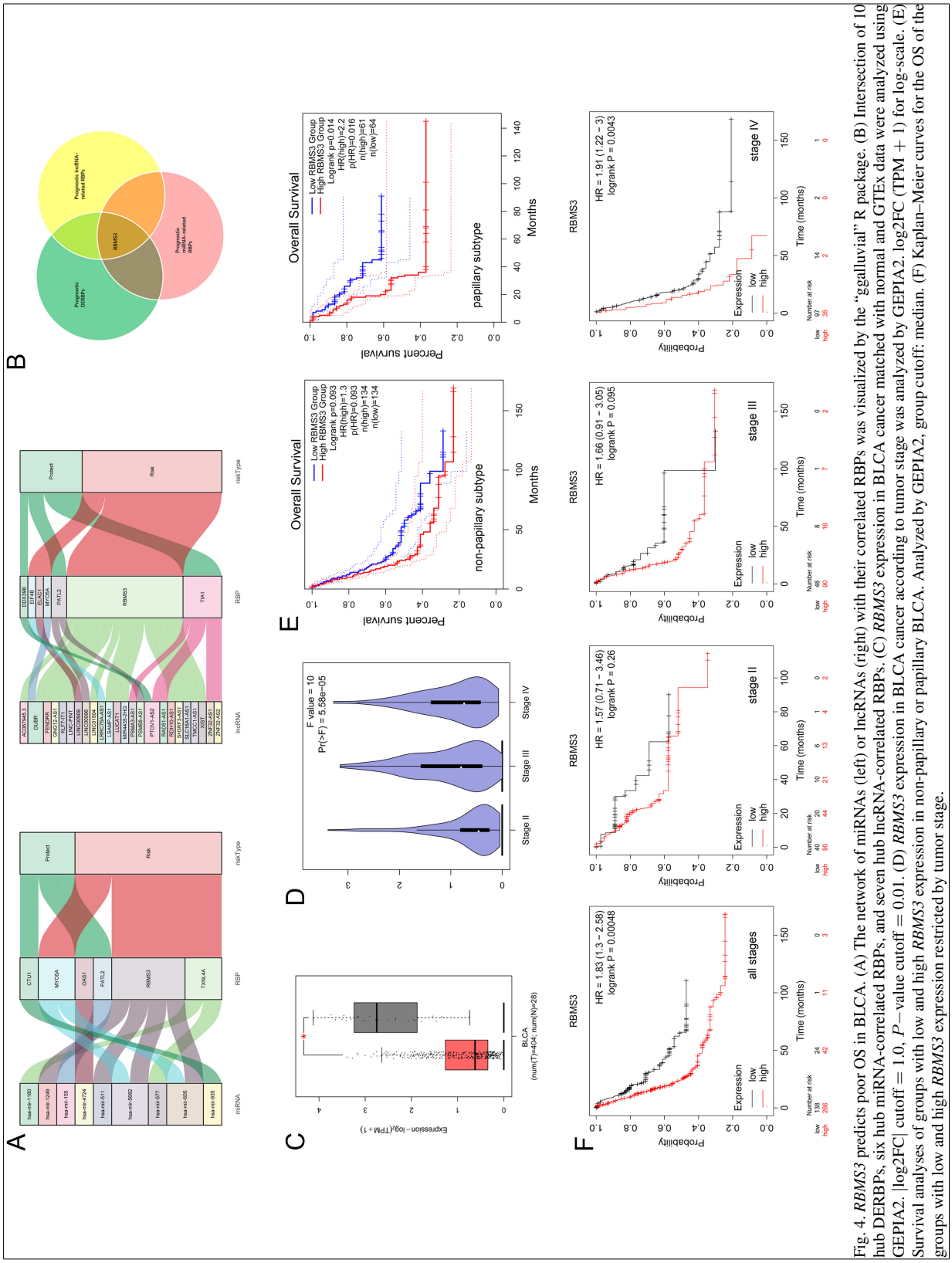

Fig. 4. *RBMS3* predicts poor OS in BLCA. (A) The network of miRNAs (left) or lncRNAs (right) with their correlated RBPs was visualized by the "ggalluvial" R package. (B) Intersection of 10 hub DERBPs, six hub miRNA-correlated RBPs, and seven hub lncRNA-correlated RBPs. (C) *RBMS3* expression in BLCA cancer matched with normal and GTEx data were analyzed using GEPIA2. $|\log2FC|$ cutoff $= 1.0$, $P-$value cutoff $= 0.01$. (D) *RBMS3* expression in BLCA cancer according to tumor stage was analyzed by GEPIA2. log2FC (TPM $+ 1$) for log-scale. (E) Survival analyses of groups with low and high *RBMS3* expression in non-papillary or papillary BLCA. Analyzed by GEPIA2, group cutoff: median. (F) Kaplan–Meier curves for the OS of the groups with low and high *RBMS3* expression restricted by tumor stage.

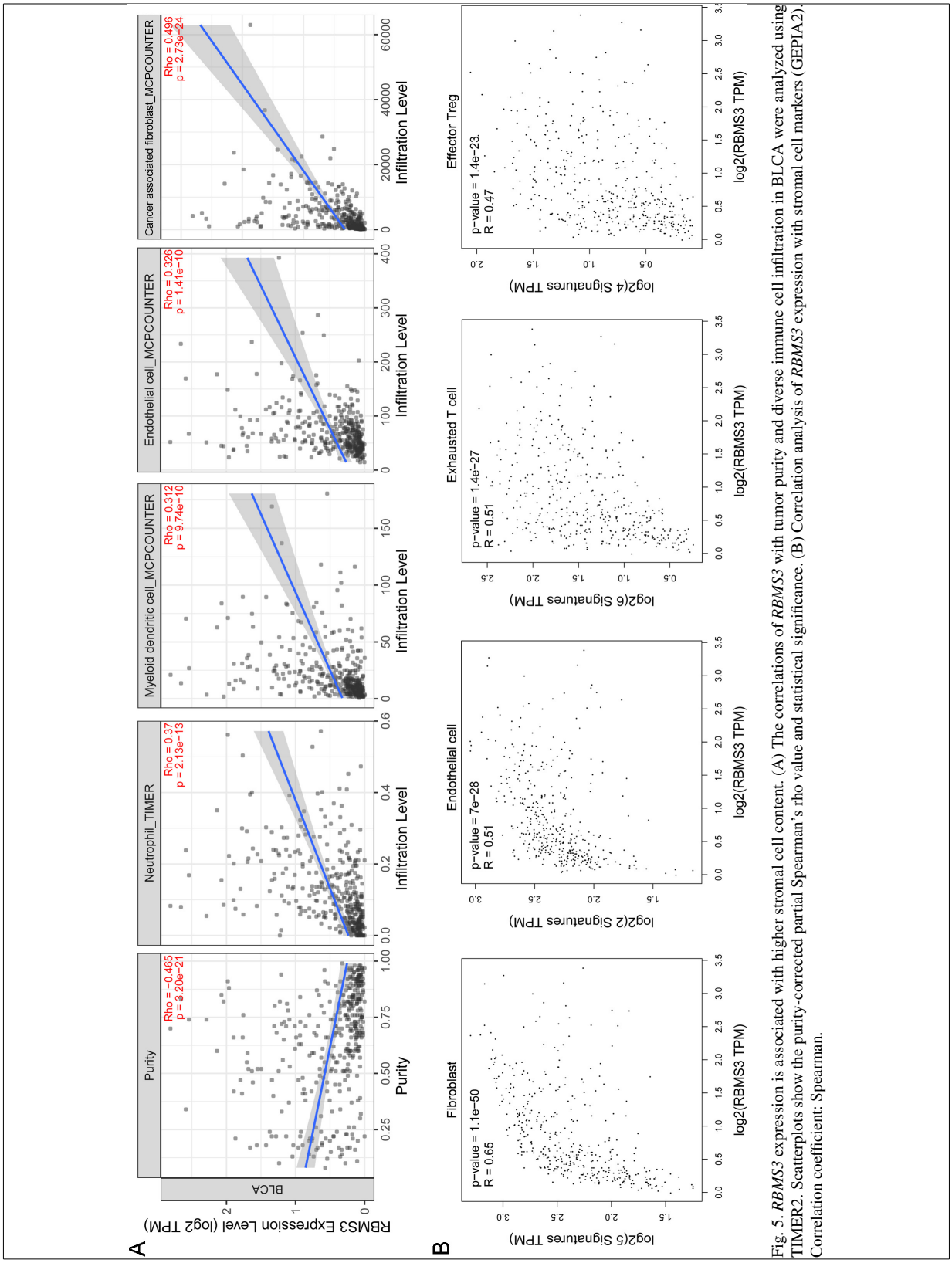

Fig. 5. *RBMS3* expression is associated with higher stromal cell content. (A) The correlations of *RBMS3* with tumor purity and diverse immune cell infiltration in BLCA were analyzed using TIMER2. Scatterplots show the purity-corrected partial Spearman's rho value and statistical significance. (B) Correlation analysis of *RBMS3* expression with stromal cell markers (GEPIA2). Correlation coefficient: Spearman.

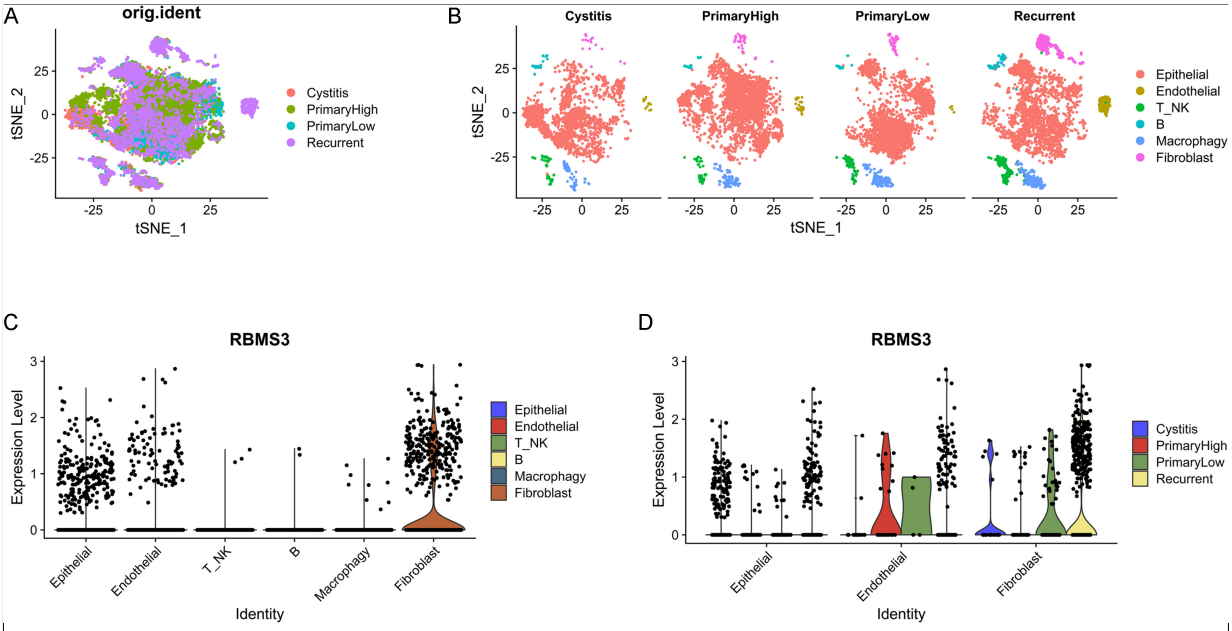

Fig. 6. *RBMS3* is mainly expressed in epithelial, endothelial, and fibroblast cells. (A) tSNE plot of cells from four patients. (B) tSNE plot of the cell clusters split according to origin. (C) VlnPlot of *RBMS3* expression according to cell type. (D) *RBMS3* expression in epithelial, endothelial, and fibroblast cells split according to origin.

3.7. High RBMS3 expression predicts poor survival in BLCA immunotherapy

The TME is an essential factor affecting immune response. As key components of the TME, cancer-associated fibroblasts play critical roles in efficient anti-programmed cell death protein 1(PD-1)/anti-programmed death ligand 1 (PD-L1) immunotherapy by participating in extracellular matrix remodeling [27, 28]. Since *RBMS3* is highly correlated with fibroblast cells and the immunosuppressive TME, we wondered whether it affects immunotherapy. Our results based on the Imvigor210CoreBiologies dataset showed that the non-response patients had higher *RBMS3* expression level than the response patients ($P = 0.0016$, Fig. 8A). Consistently, high *RBMS3* expression group contained more non-response patients (85%) than low *RBMS3* expression group (70%, Fig. 8B). Additionally, patients with high *RBMS3* expression exhibited significantly worse OS compared to those with low *RBMS3* expression ($P = 0.0033$, Fig. 8C).

We further analyzed the predictive value of RBMS3 on BLCA immunotherapy through the Kaplan-Meier Plotter. Results showed that high *RBMS3* expression was a risk factor for anti–PD-1 (HR = 3.25, $P = 0.051$) immunotherapy in BLCA patients (Fig. 8D). *RBMS3* also associated with a lower survival probability for anti–PD-L1 immunotherapy, but with no statistical difference ($P = 0.27$, Fig. 8E). This may be because of the small size of the BLCA sample ($n = 90$). In a large urothelial carcinoma cohort ($n = 348$) that received anti–PD-L1 immunotherapy, a significant survival difference was noted between the groups with low and high RBMS3 expression (Fig. 8F). All the results suggested that RBMS3 may predict the efficacy of BLCA immunotherapy.

4. Discussion

Risk stratification of cancer traditionally uses clinical and pathological characteristics to provide prognostic information, helping to select the best treatment for each patient [4]. Epidemiologically, advanced age, cigarette smoking, and heredity are the risk factors for BLCA [2]. Based on genetic alterations in the DNA and subsequent RNA expression levels, BLCA can be grouped into distinct molecular subtypes with variable prognostic, predictive, and therapeutic implications [2]. Increasing evidence indicates that RBPs play a crucial role in the initiation, development, and recurrence of various malignant tumors [29]. Several studies have identified risk RBP signatures in BLCA [17,18,19]. In this study, we established a risk score model based on DERBPs. Moreover, we successfully constructed a nomogram combining the risk score with clinical vari-

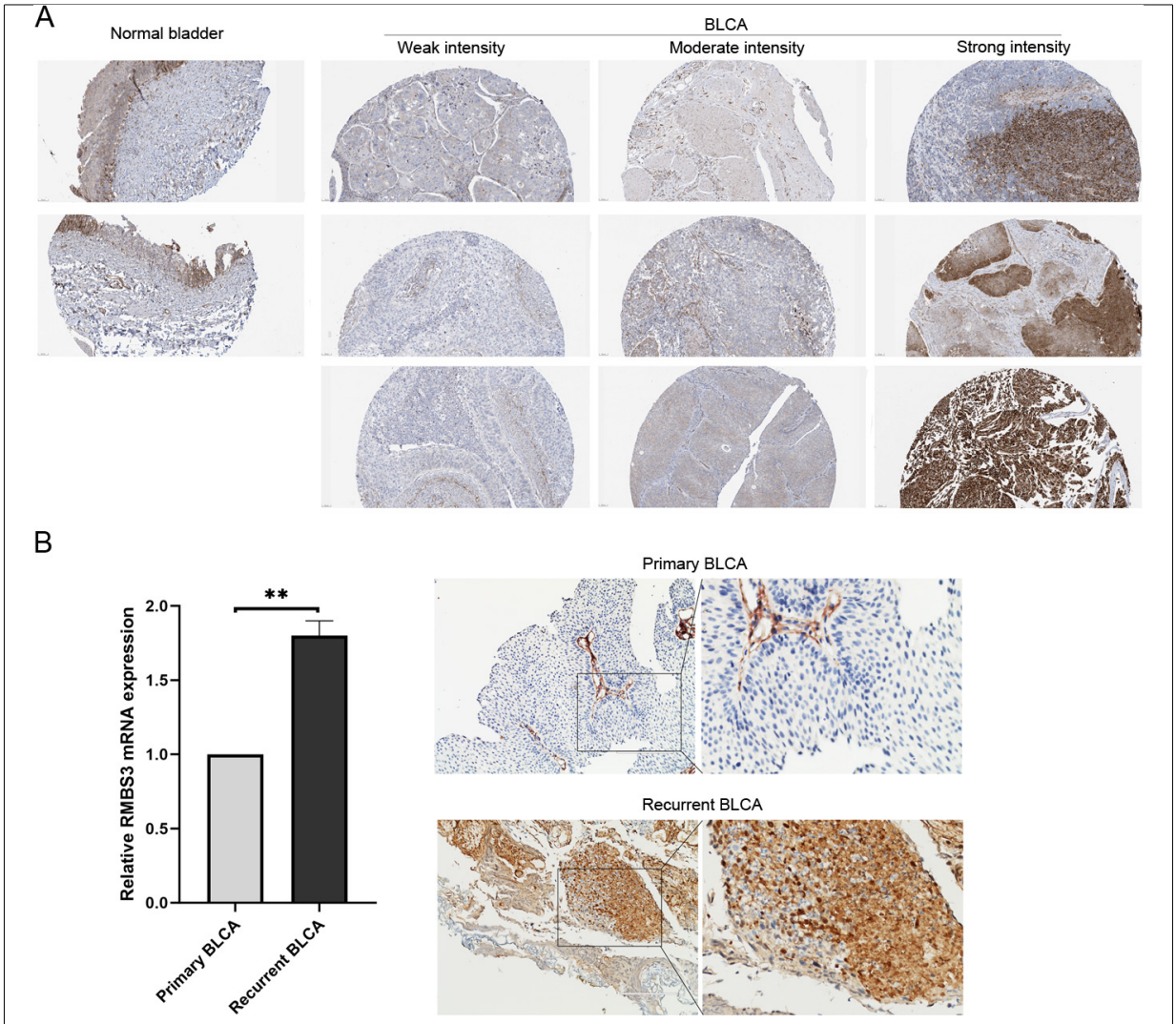

Fig. 7. RBMS3 expression in BLCA tissue. (A)The immunohistochemistry results of RBMS3 protein in normal bladder and BLCA tissues from the Human Protein Atlas. (B) In the primary and recurrent BLCA tissues, RBMS3 mRNA level was examined by quantitative real-time PCR, $^{**}P < 0.01$ (left), RBMS3 protein was detected by immunohistochemistry assay.

ables to establish a quantitative prognostic evaluation of the OS of BLCA patients. High-risk patients showed increased stromal scores and differential immune cell infiltration compared to low-risk patients. These results indicate that prognostic RBPs participate in the malignant progression of BLCA by functioning as regulators of tumor stromal content.

RBPs establish highly dynamic interactions with coding and non-coding RNAs to regulate RNA splicing, stability, localization, translation, and degradation [29]. Therefore, critical RBPs that participate in the malignant progression of BLCA should be correlated with RNA expression. To further explore the critical RBPs for cancer development, we additionally identified RNA-correlated RBPs with prognostic value – namely, prognostic miRNA-correlated RBPs and prognostic lncRNA-correlated RBPs. After intersection, *RBMS3* was found to be the only gene present in all three prognostic RBP signatures. We noticed that RBMS3 was also included in the prognostic RBP signature in previous studies [18,19]. This finding highlights the importance of RBMS3 in the development of BLCAs.

RBMS3 expression was downregulated in BLCA tissues compared to normal bladder samples. However, in BLCA samples collected at different tumor stages, RBMS3 was upregulated at relatively more advanced stages of BLCA. These contradictory find-

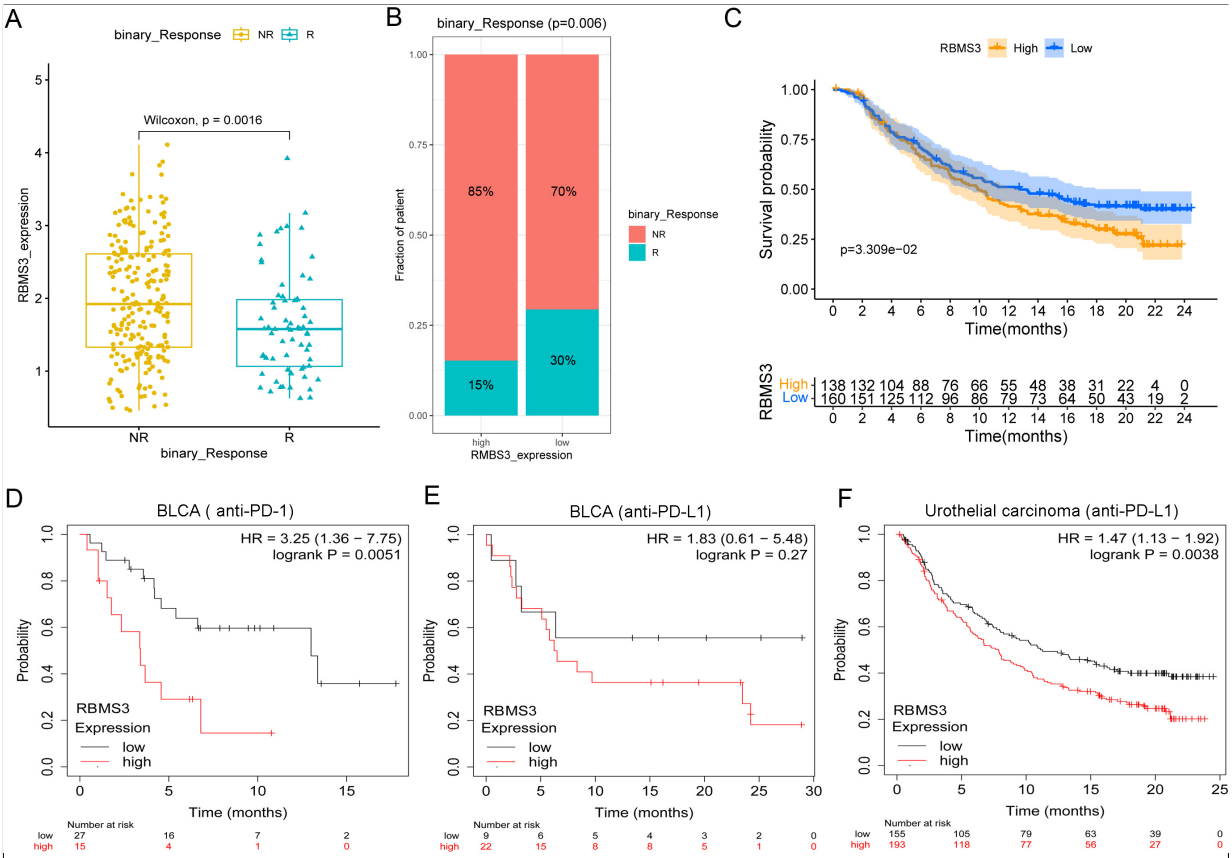

Fig. 8. High *RBMS3* expression predicts poor response to BLCA immunotherapy. (A–C) Exploration of *RBMS3* expression as prognostic markers for BLCA immunotherapy (immune checkpoint inhibitors) using the Imvigor210CoreBiologies dataset. (A) Difference of *RBMS3* expression between different immune response patients, NR: non-response, R: response. (B) Comparison of immune response ratio between high- and low-RBMS3 expression patients. (C) Survival analysis of high- and low-RBMS3 expression patients. (D–F) Survival analysis of the high- and low-RBMS3 expression BLCA patients received immune checkpoint inhibitors treatment using the Kaplan-Meier Plotter. (D) Kaplan–Meier plot of anti–PD-1 and (E) anti–PD-L1 immunotherapy in BLCA ($n = 90$). (F) Kaplan–Meier plot of anti–PD-L1 immunotherapy in urothelial carcinoma ($n = 348$). Cutoff: auto-select.

ings have been observed for several genes. For example, the ferroptosis-related gene *CHAC1* is downregulated in kidney renal clear cell carcinoma but shows increased expression in more malignant kidney renal clear cell carcinoma samples and is associated with poor OS [30]. Pleiotrophin mRNA levels in many breast cancer samples are not higher than normal levels; however, pleiotrophin also positively regulates growth, angiogenesis, and chemoresistance in breast cancer [31]. A reasonable explanation is that these genes may participate in malignant progression instead of cancer initiation [30]. In this study, *RBMS3* expression was associated with poor OS in BLCA patients. Survival analysis restricted to the tumor subtype revealed that high RBMS3 expression was a risk factor for papillary BLCA but not for non-papillary BLCA. Moreover, the survival disadvantage is obvious in stage IV BLCA but not in lower-stage (II and III) BLCA. These results suggest an important contribution of RBMS3 to the malignant progression of BLCA, especially papillary BLCA.

By reviewing the existing literature, we noticed that RBMS3 can exert both pro- and anti-cancer effects in different types of cancers. First, RBMS3 was identified as a tumor-suppressive gene during tumorigenesis. RBMS3 effectively suppressed the tumorigenicity of esophageal squamous cell carcinoma cells by downregulating C-MYC [32]. Consistently, another study reported that the loss of RBMS3 cooperates with the oncoprotein $BRAF^{V600E}$ to induce lung tumorigenesis [33]. Silencing of RBMS3 promotes the growth of $BRAF^{V600E}$ lung organoids and the development of malignant lung cancers by elevating the Wnt/β-catenin signaling axis [33]. RBMS3 negatively regulates chemo-

resistance in epithelial ovarian cancer. Genetic ablation of RBMS3 significantly enhanced the chemo-resistance of epithelial ovarian cancer cells [34]. More recently, it has been shown that RBMS3 expression plays a tumor suppressor role in epithelial ovarian cancer by inducing an immune promoting TME [35]. RBMS3 showed a negatively correlation with markers of regulatory T cell, myeloid-derived suppressor cell, and M2 macrophage but a positive correlation with markers of M1 macrophage [35]. These studies suggest that RBMS3 has tumor-suppressive functions in certain type of cancers.

However, recent studies have shown that RBMS3 has cancer-promoting potential, which is necessary for malignant progression [36]. The most well-studied cancer-promoting potential of RBMS3 concerns the epithelial-mesenchymal transition (EMT) relationship [37]. RBMS3 expression is positively associated with EMT. According to prior research, RBMS3 is necessary for maintaining the mesenchymal phenotype and invasion in triple-negative breast cancer models [38]. Loss of RBMS3 significantly impairs tumor progression and spontaneous metastasis in vivo [38]. Functionally, RBMS3 interacts with and stabilizes the mRNA PRRX1 (an EMT transcription factor) [38]. The EMT-promoting function of RBMS3 may explain its upregulation in advanced tumors and its association with poor survival.

In the present study, RBMS3 expression was associated with a higher stromal score. Specifically, RBMS3 expression was highly correlated with counts of fibroblasts. Using scRNA-Seq analysis, it was also revealed that RBMS3 is highly expressed in fibroblasts and endothelial cells in BLCA tissues, while immunohistochemical analysis from the Human Protein Atlas confirmed that high levels of RBMS3 were observed in the tumor stromal area in some BLCA tissues. Similar results have been reported for breast cancer: higher RBMS3 expression was observed in breast cancer stromal cells compared to tumor cells [36]. Therefore, RBMS3 may be enriched in tumor stromal cells, thereby participating in TME remodeling. The immunosuppressive TME is a major obstacle to efficient anti-cancer immunotherapy [28]. According to the infiltration pattern of immune cells, tumors are commonly classified into three categories – namely, "inflamed", "immune-excluded", and "immune desert" [39]. Most BLCA tumors (approximately 47%) are immune-excluded and show a lower response to immune checkpoint inhibitors [40]. Abnormal activation of tumor-associated fibroblasts plays a critical role in immune-excluded BLCA tumors [40]. In this study, RBMS3 was highly correlated with fibroblast cells and the immunosuppressive TME. Moreover, the Kaplan–Meier plot demonstrated that high RBMS3 expression is a risk factor for immunotherapy in patients with BLCA. Actually, RBMS3 has been reported to be a target to improve anti-cancer immunity in triple-negative breast cancer. *RBMS3* correlates with several immunosuppressive molecules such as CD274. Mechanistically, RBMS3 protein binds to CD274 mRNA specifically to increase PD-L1 levels. Disruption of RBMS3 can enhance the anti-tumor immune activity by suppressing PD-L1 [41]. Collectively, these results highlight the role of RBMS3 in promoting an immunosuppressive TME in BLCA.

This study had some limitations. Most results of this were gleaned from public databases, and additional *in vitro* and *in vivo* studies are needed to prove the mechanism of action of RBMS3 in BLCA. TCGA was the main database used in this study, additional well-developed datasets were required to validate the main findings.

In conclusion, we constructed three prognostic RBPs signatures based on DERBPs, miRNA-correlated RBPs, and lncRNA-correlated RBPs in BLCA. RBMS3 has been identified as a key prognostic gene with TME remodeling functions. The potent role of RBMS3 in the immunosuppressive TME provides a foundation and new ideas for BLCA immunotherapy.

Declaration of interests

The authors declare that they have no known competing financial interests or personal relationships that could influence the work reported in this study.

Author contributions

All authors listed have made a substantial contribution to this work and approved the manuscript. Conception: Jinlong Li and Li Zhou; interpretation or analysis of data: Tarimo Fredrick Praygod and Zhiming Hu; preparation of the manuscript: Li Zhou and Tarimo Fredrick Praygod ; revision for important intellectual content: Hongwei Li and Tan Wanlong; supervision: Jinlong Li.

Acknowledgments

This study was supported by a grant from the Natural Science Foundation of Guangdong Province

(No.2022A1515010515) and Heyuan City Science and Technology Plan Project (No. Heke Platform 007).

Supplementary data

The supplementary files are available to download from http://dx.doi.org/10.3233/CBM-230489.

References

[1] H. Sung, J. Ferlay, R.L. Siegel, M. Laversanne, I. Soerjomataram, A. Jemal and F. Bray, Global cancer statistics 2020: GLOBOCAN estimates of incidence and mortality worldwide for 36 cancers in 185 countries, *CA Cancer J Clin* **71** (2021), 209–249.

[2] A.T. Lenis, P.M. Lec, K. Chamie and M.D. Mshs, Bladder cancer: A review, *JAMA* **324** (2020), 1980–1991.

[3] D.J. McConkey and W. Choi, Molecular subtypes of bladder cancer, *Curr Oncol Rep* **20** (2018), 77.

[4] J.T. Matulay and A.M. Kamat, Advances in risk stratification of bladder cancer to guide personalized medicine, *F1000Res* **7** (2018).

[5] S. Gerstberger, M. Hafner and T. Tuschl, A census of human RNA-binding proteins, *Nat Rev Genet* **15** (2014), 829–45.

[6] D. Kang, Y. Lee and J.S. Lee, RNA-binding proteins in cancer: Functional and therapeutic perspectives, *Cancers (Basel)* **12** (2020).

[7] S. Wang, Z. Sun, Z. Lei and H.T. Zhang, RNA-binding proteins and cancer metastasis, *Semin Cancer Biol* **86** (2022), 748–768.

[8] Y. Zhang, Y. Zhang, J. Song, X. Cheng, C. Zhou, S. Huang, W. Zhao, Z. Zong and L. Yang, Targeting the "tumor microenvironment": RNA-binding proteins in the spotlight in colorectal cancer therapy, *Int Immunopharmacol* **131** (2024), 111876.

[9] Q. Liao and J. Xiong, YTHDF1 regulates immune cell infiltration in gastric cancer via interaction with p53, *Exp Ther Med* **27** (2024), 255.

[10] C. Chen, C. Wang, W. Liu, J. Chen, L. Chen, X. Luo and J. Wu, Prognostic value and gene regulatory network of CMSS1 in hepatocellular carcinoma, *Cancer Biomark* **39** (2024), 361–370.

[11] W. Pan, X. Liu and S. Liu, ALYREF m5C RNA methylation reader predicts bladder cancer prognosis by regulating the tumor immune microenvironment, *Medicine (Baltimore)* **103** (2024), e37590.

[12] Y. Huang, S. Chen, W. Qin, Y. Wang, L. Li, Q. Li and X. Yuan, A novel RNA binding protein-related prognostic signature for hepatocellular carcinoma, *Front Oncol* **10** (2020), 580513.

[13] L. Xu, W. Li, T. Yang, S. Hu, Q. Zou, J. Jiao, N. Jiang and Y. Zhang, Immune-related RNA-binding protein-based signature with predictive and prognostic implications in patients with lung adenocarcinoma, *Front Mol Biosci* **9** (2022), 807622.

[14] J. Zhang, X. Miao, T. Wu, J. Jia and X. Cheng, Development and validation of Ten-RNA binding protein signature predicts overall survival in osteosarcoma, *Front Mol Biosci* **8** (2021), 751842.

[15] R. Ming, X. Li, E. Wang, J. Wei, B. Liu, P. Zhou, W. Yu, S. Zong and H. Xiao, The prognostic signature of head and neck squamous cell carcinoma constructed by immune-related RNA-binding proteins, *Front Oncol* **12** (2022), 795781.

[16] S. Yang, S. Lin, K. Liu, Y. Liu, P. Xu, Y. Zheng, Y. Deng, D. Zhang, Z. Zhai, N. Li, X. Ren, Z. Dai and H. Kang, Identification of an immune-related RNA-binding protein signature to predict survival and targeted therapy responses in liver cancer, *Genomics* **113** (2021), 795–804.

[17] Y. Wu, Y. Liu, A. He, B. Guan, S. He, C. Zhang, Z. Kang, Y. Gong, X. Li and L. Zhou, Identification of the six-RNA-binding protein signature for prognosis prediction in bladder cancer, *Front Genet* **11** (2020), 992.

[18] F. Chen, Q. Wang and Y. Zhou, The construction and validation of an RNA binding protein-related prognostic model for bladder cancer, *BMC Cancer* **21** (2021), 244.

[19] Y. Wu, Z. Liu, X. Wei, H. Feng, B. Hu, B. Liu, Y. Luan, Y. Ruan, X. Liu, Z. Liu, S. Wang, J. Liu and T. Wang, Identification of the functions and prognostic values of RNA binding proteins in bladder cancer, *Front Genet* **12** (2021), 574196.

[20] K.B. Cook, H. Kazan, K. Zuberi, Q. Morris and T.R. Hughes, RBPDB: a database of RNA-binding specificities, *Nucleic Acids Res* **39** (2011), D301–8.

[21] A.G. Baltz, M. Munschauer, B. Schwanhausser, A. Vasile, Y. Murakawa, M. Schueler, N. Youngs, D. Penfold-Brown, K. Drew, M. Milek, E. Wyler, R. Bonneau, M. Selbach, C. Dieterich and M. Landthaler, The mRNA-bound proteome and its global occupancy profile on protein-coding transcripts, *Mol Cell* **46** (2012), 674–90.

[22] S.C. Kwon, H. Yi, K. Eichelbaum, S. Fohr, B. Fischer, K.T. You, A. Castello, J. Krijgsveld, M.W. Hentze and V.N. Kim, The RNA-binding protein repertoire of embryonic stem cells, *Nat Struct Mol Biol* **20** (2013), 1122–30.

[23] J. Fang, F. Chen, D. Liu, F. Gu, Z. Chen and Y. Wang, Prognostic value of immune checkpoint molecules in breast cancer, *Biosci Rep* **40** (2020).

[24] X. Qu, X. Zhao, K. Lin, N. Wang, X. Li, S. Li, L. Zhang and Y. Shi, M2-like tumor-associated macrophage-related biomarkers to construct a novel prognostic signature, reveal the immune landscape, and screen drugs in hepatocellular carcinoma, *Front Immunol* **13** (2022), 994019.

[25] Z. Tang, B. Kang, C. Li, T. Chen and Z. Zhang, GEPIA2: An enhanced web server for large-scale expression profiling and interactive analysis, *Nucleic Acids Res* **47** (2019), W556–W560.

[26] T. Zhang, Y. Wu, Z. Fang, Q. Yan, S. Zhang, R. Sun, J. Khaliq and Y. Li, Low expression of RBMS3 and SFRP1 are associated with poor prognosis in patients with gastric cancer, *Am J Cancer Res* **6** (2016), 2679–2689.

[27] L. Pei, Y. Liu, L. Liu, S. Gao, X. Gao, Y. Feng, Z. Sun, Y. Zhang and C. Wang, Roles of cancer-associated fibroblasts (CAFs) in anti- PD-1/PD-L1 immunotherapy for solid cancers, *Mol Cancer* **22** (2023), 29.

[28] X. Mao, J. Xu, W. Wang, C. Liang, J. Hua, J. Liu, B. Zhang, Q. Meng, X. Yu and S. Shi, Crosstalk between cancer-associated fibroblasts and immune cells in the tumor microenvironment: new findings and future perspectives, *Mol Cancer* **20** (2021), 131.

[29] B. Pereira, M. Billaud and R. Almeida, RNA-binding proteins in cancer: Old players and new actors, *Trends Cancer* **3** (2017), 506–528.

[30] D. Li, S. Liu, J. Xu, L. Chen, C. Xu, F. Chen, Z. Xu, Y. Zhang, S. Xia, Y. Shao and Y. Wang, Ferroptosis-related gene CHAC1 is a valid indicator for the poor prognosis of kidney renal clear cell carcinoma, *J Cell Mol Med* **25** (2021), 3610–3621.

[31] X. Wang, Pleiotrophin: Activity and mechanism, *Adv Clin Chem* **98** (2020), 51–89.

[32] Y. Li, L. Chen, C.J. Nie, T.T. Zeng, H. Liu, X. Mao, Y. Qin, Y.H. Zhu, L. Fu and X.Y. Guan, Downregulation of RBMS3 is

associated with poor prognosis in esophageal squamous cell carcinoma, *Cancer Res* **71** (2011), 6106–15.

[33] A. Vaishnavi, J. Juan, M. Jacob, C. Stehn, E.E. Gardner, M.T. Scherzer, S. Schuman, J.E. Van Veen, B. Murphy, C.S. Hackett, A.J. Dupuy, S.A. Chmura, L. van der Weyden, J.Y. Newberg, A. Liu, K. Mann, A.G. Rust, W.A. Weiss, C.G. Kinsey, D.J. Adams, A. Grossmann, M.B. Mann and M. McMahon, Transposon mutagenesis reveals RBMS3 silencing as a promoter of malignant progression of BRAFV600E-Driven lung tumorigenesis, *Cancer Res* **82** (2022), 4261–4273.

[34] G. Wu, L. Cao, J. Zhu, Z. Tan, M. Tang, Z. Li, Y. Hu, R. Yu, S. Zhang, L. Song and J. Li, Loss of RBMS3 confers platinum resistance in epithelial ovarian cancer via activation of miR-126-5p/beta-catenin/CBP signaling, *Clin Cancer Res* **25** (2019), 1022–1035.

[35] T. Yin, Y. Zhang, Y. Zhao, X. Zhang, S. Han, Y. Wang and B. Yang, Tumor suppressor function of RBMS3 overexpression in EOC associated with immune cell infiltration, *Heliyon* **10** (2024), e30603.

[36] T. Gornicki, J. Lambrinow, M. Mrozowska, H. Romanowicz, B. Smolarz, A. Piotrowska, A. Gomulkiewicz, M. Podhorska-Okolow, P. Dziegiel and J. Grzegrzolka, Expression of RBMS3 in Breast Cancer Progression, *Int J Mol Sci* **24** (2023).

[37] T. Gornicki, J. Lambrinow, M. Mrozowska, M. Podhorska-Okolow, P. Dziegiel and J. Grzegrzolka, Role of RBMS3 novel potential regulator of the EMT phenomenon in physiological and pathological processes, *Int J Mol Sci* **23** (2022).

[38] C.J. Block, A.V. Mitchell, L. Wu, J. Glassbrook, D. Craig, W. Chen, G. Dyson, D. DeGracia, L. Polin, M. Ratnam, H. Gibson and G. Wu, RNA binding protein RBMS3 is a common EMT effector that modulates triple-negative breast cancer progression via stabilizing PRRX1 mRNA, *Oncogene* **40** (2021), 6430–6442.

[39] P.S. Hegde and D.S. Chen, Top 10 Challenges in Cancer Immunotherapy, *Immunity* **52** (2020), 17–35.

[40] S. Mariathasan, S.J. Turley, D. Nickles, A. Castiglioni, K. Yuen, Y. Wang, E.E. Kadel, III, H. Koeppen, J.L. Astarita, R. Cubas, S. Jhunjhunwala, R. Banchereau, Y. Yang, Y. Guan, C. Chalouni, J. Ziai, Y. Senbabaoglu, S. Santoro, D. Sheinson, J. Hung, J.M. Giltnane, A.A. Pierce, K. Mesh, S. Lianoglou, J. Riegler, R.A.D. Carano, P. Eriksson, M. Hoglund, L. Somarriba, D.L. Halligan, M.S. van der Heijden, Y. Loriot, J.E. Rosenberg, L. Fong, I. Mellman, D.S. Chen, M. Green, C. Derleth, G.D. Fine, P.S. Hegde, R. Bourgon and T. Powles, TGFbeta attenuates tumour response to PD-L1 blockade by contributing to exclusion of T cells, *Nature* **554** (2018), 544–548.

[41] Y. Zhou, Z. Liang, Y. Xia, S. Li, J. Liang, Z. Hu, C. Tang, Q. Zhao, Q. Gong and Y. Ouyang, Disruption of RBMS3 suppresses PD-L1 and enhances antitumor immune activities and therapeutic effects of auranofin against triple-negative breast cancer, *Chem Biol Interact* **369** (2023), 110260.